https://doi.org/10.30799/jnst.098.18040104 J. Nanosci. Tech. - Volume 4 Issue 1 (2018) 314–316

Share Your Innovations through JACS Directory

Journal of Nanoscience and Technology

Visit Journal at http://www.jacsdirectory.com/jnst

ISSN: 2455-0191

A Comparable Study of Structural, Dielectric and Humidity Sensing Properties of Solution Combustion Synthesized ZrO_2 and $ZrTiO_4$ Nano Powders

H.C. Madhusudhana[1,2,*], S.N. Shobhadevi[3], B.M. Nagabhushana[4], M.V. Murugendrappa[5], R. Hari Krishna[4], H. Nagabhushana[6]

[1]*Department of Physics, Dayananda Sagar Academy of Technology and Management, Bangalore – 560 082, Karnataka, India.*
[2] *BMS Academy of Science and Research, Tumkur University, Tumkur – 572 103, Karnataka, India.*
[3]*Department of Physics, B. M. S. College for Women, Bangalore – 560 004, Karnataka, India.*
[4]*Department of Chemistry, M. S. Ramaiah Institute of Technology, Bangalore – 560 054, Karnataka, India.*
[5]*Department of Physics, BMS College of Engineering, Bangalore – 560 019, Karnataka, India.*
[6]*C.N.R.Center for Nano Research, Tumkur University, Tumkur – 572 103, Karnataka, India.*

ARTICLE DETAILS

Article history:
Received 17 February 2018
Accepted 25 February 2018
Available online 28 February 2018

Keywords:
$ZrTiO_4$
Combustion
Dielectric Constant

ABSTRACT

Simple and cost-effective solution combustion method is used to synthesize nano powders of ZrO_2 and $ZrTiO_4$. The structural and morphological analysis was done by X-ray diffraction (XRD) and scanning electron microscopy (SEM). Results revealing the phase confirmation and structure of synthesized samples. Dielectric properties of the synthesized $ZrTiO_4$ powder dominates the synthesized ZrO_2 having superior dielectric constant ($\varepsilon' = 50$), Low dielectric loss and enhanced conductivity ($\sigma_{ac} = 2.75 \times 10^{-4}$ Scm^{-1}) at room temperature. The humidity sensing properties for $ZrTiO_4$ shows good linear behavior compare to ZrO_2.

1. Introduction

$ZrTiO_4$ is a class ceramic material with excellent thermal and electrical properties and poses high resistance to heat and corrosive environment. $ZrTiO_4$ is widely used to manufacture electrical and optical devices, such as capacitors, piezoelectric sensors, ultrasonic motors and dielectric devices in microwaves, since it presents high permittivity in the microwave frequency [1, 2]. The traditional preparation of ZT ceramics is based on solid state reactions between the TiO_2 and $ZrTiO_4$ powders at high temperatures (1400 °C). In order to improve the functional properties of the ceramic material, treatments consuming a high amount of energy after the reaction are generally necessary and expensive [3]. Chemical methods based on co-precipitation of the reactive precursors were developed to prepare powders with a high purity and low treatment cost after a reaction [4, 5]. $ZrTiO_4$ crystallizes in the orthorhombic type structure α-PbO_2. This phase is stable above 1100 °C and persists metastably at low temperature because the ordering process is sluggish, being associated with a reconstructive transformation. Samples containing multi-phases are important from the technological perspective and are strongly superposed [6]. Consentino et al. [7] prepared ceramic powders from the mixture of zirconium oxychloride and titanium chloride in stoichiometric quantities in the presence of citric acid. At the present work we prepare $ZrTiO_4$ nano crystals with multi phases by solution combustion method by using Glycine as a fuel and we are comparing the results with ZrO_2 prepared by solution combustion method as prepared earlier by few workers [8]. The obtained samples are analyzed by XRD, SEM, AC conductivity and humidity sensing properties.

2. Experimental Methods

2.1 Synthesis

Glycine ($C_2H_5NO_2$) was used as fuel to synthesize both ZrO_2 and $ZrTiO_4$ nano powders by solution combustion method. To synthesize ZrO_2 we followed the same procedure as we did earlier [8]. To synthesize $ZrTiO_4$ nano powder Titanium nitrate [$TiO(NO_3)_2$] and Zirconyl nitrate [$ZrO(NO_3)_2.XH_2O$] (Central Drug House (P) Ltd.) were used as oxidizers. Now, both the chemicals were dissolved in 25 mL of deionized water. Stoichiometric composition of the redox mixtures was calculated based on the total oxidizing and reducing valences of the oxidizer (O) and the fuel (F) keeping the O/F ratio as unity. The aqueous solution containing the redox mixture was taken in a crystalline dish and introduced in a preheated muffle furnace maintained at 500 °C to obtain a milky precipitate. The reaction involved within the precipitate start giving the sparks resulting in the formation of $ZrTiO_4$ white nano powder. The process is called smoldering combustion. During the course of this reaction, temperature was exceeding 1000 °C. At the end of this period, the $ZrTiO_4$ white nano powder was formed. The combustion synthesis process was completed with the total time span of 5 minutes. The obtained $ZrTiO_4$ nano powder was grinded well as a fine powder. The obtained nano powder is calcinated at 900 °C for 3 hours. Assuming the complete combustion, the theoretical equations for the formation of ZrO_2 and $ZrTiO_4$ with Glycine can be written as follows:

For ZrO_2 synthesis:

$$ZrO(NO_3)_2 + 2C_2H_5NO_2 \rightarrow ZrO_2 + 2N_2 + 4CO_2 + 5H_2O$$

For $ZrTiO_4$ synthesis:

$$9ZrO(NO_3)_2 + 9TiO(NO_3)_2 + 20C_2H_5NO_2 \rightarrow 9ZrTiO_4 + 50H_2O + 28N_2 + 40CO_2$$

2.2 Characterization

The X-ray diffraction patterns of both ZrO_2 and $ZrTiO_4$ were recorded on X-ray diffractometer (Bruker AXS D8 Advance) using Cuk_α radiation (λ=1.5418 Å) in the 2θ range 20° - 80°. The FTIR spectra of the $ZrTiO_4$ were

*Corresponding Author: msudhan01@gmail.com(H.C. Madhusudhana)

https://doi.org/10.30799/jnst.098.18040104

Cite this Article as: H.C. Madhusudhana, S.N. Shobhadevi, B.M. Nagabhushana, M.V. Murugendrappa, R. Hari Krishna, H. Nagabhushana, A comparable study of structural, dielectric and humidity sensing properties of solution combustion synthesized ZrO_2 and $ZrTiO_4$ nano powders, J. Nanosci. Tech. 4(1) (2018) 314–316.

recorded on IR Affinity-1 (Shimadzu, Japan) spectrometer in KBr medium, at room temperature and the SEM micrographs were studied using Scanning Electron Microscope (Jeol 6390 LV). The 6500B series of Precision Impedance Analyzers (Wayne Kerr-UK Electronics Pvt. Ltd., India) was used for the measurement of conductivity parameters, in the frequency range from 100 Hz to 10^6 Hz at room temperature for the samples. The humidity response measurements were done by Humidity Sensor (V B Ceramic Consultant, Chennai, India) for the both samples in the cooling temperature range between 70 °C and 0 °C.

3. Results and Discussion

3.1 XRD Analysis

XRD Characterization is done using with CuK_α radiation = 1.5418 Å. These X-rays are collimated and directed onto the sample. As the sample and detector are rotated, the intensity of the reflected X-rays is recorded. When the geometry of the incident X-rays impinging the sample satisfies the Bragg equation, constructive interference occurs and a peak in intensity occurs. The formation of crystalline phase prepared by solution combustion (SC) method is confirmed by PXRD measurement. Fig. 1 shows the X-ray diffraction patterns of both ZrO_2 and $ZrTiO_4$. ZrO_2 shows pure phase belongs to tetragonal phase (JCPDS card No. 80-0965) and $ZrTiO_4$ shows its formation orthorhombic phase (JCPDS card No.34-415) with traces of ZrO_2 and TiO_2 mixed phases. The similar results are reported by Dondi et al. [9]. The crystallite size is estimated for the powder from the full width half maximum (β) of the diffraction peaks, using Debye–Scherrer's method [10]. $D = k\lambda/\beta\cos\theta$, where 'λ' is the wavelength of X-ray (1.542 Å) 'θ' the Bragg's angle, 'k' is the constant depends on the grain shape (0.94). To verify this we followed a method suggested by Williamson and Hall (W-H) [11]. The estimated crystallite sizes are listed in the Table 1.

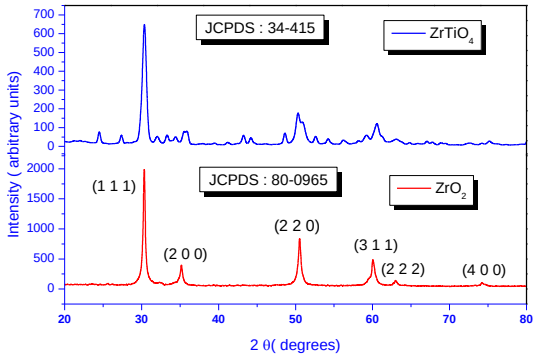

Fig. 1 XRD patterns of ZrO_2 and $ZrTiO_4$

Table 1 The estimated crystallite sizes of ZrO_2 and $ZrTiO_4$ nanopowder

Samples	Crystallite size (nm)		Strain (10^{-4})
	Scherrer's method (nm)	W-H plots (nm)	
ZrO_2(Glycine)	26	28	16
$ZrTiO_4$ (Glycine)	19	23	20

3.2 SEM Analysis

The SEM micrographs of both ZrO_2 and $ZrTiO_4$ powders are given in the Fig. 2. In general, the particles are highly porous and spike like structures whereas $ZrTiO_4$ particles are agglomerated and irregular in shape, with a substantial variation in particle size and morphology. A detailed study of higher magnification shows voids and pores of the sample. The obtained results are in agreement with reported values [7].

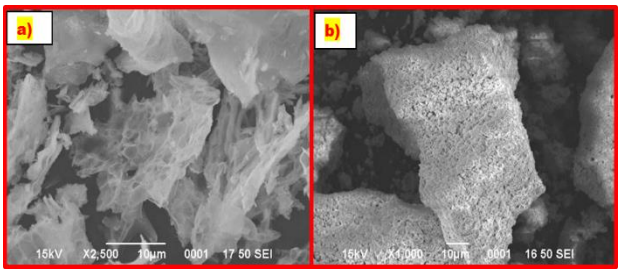

Fig. 2 SEM images of a) ZrO_2 and b) $ZrTiO_4$

3.3 Dielectric Properties

The dielectric properties of the ceramic materials are very important to study because of its excellent application in solid-state electronics [12]. The interests in studying dielectric properties are dielectric constant, dielectric loss and dielectric conductivity. For a ceramic material frequency range and environmental conditions play a vital role in dielectric behavior. It has been reported that alternating current as a function of frequency reveals valuable information about the dynamic response of the system and makes it to characterize many materials [13]. In order to investigate the properties, sintered pellets of samples are taken. These pellets were coated on both sides with silver paste.

The complex dielectric constant is given by the equation $\varepsilon = \varepsilon' - j\,\varepsilon''$ where ε' is real part of dielectric constant and ε" is imaginary part of dielectric constant.

$$\varepsilon' = \frac{C\,d}{\varepsilon_o A}; \qquad \varepsilon'' = \varepsilon' \tan\delta$$

where C is the capacitance, d is the thickness and A is the cross sectional area of the sample. ε_0 is the relative permittivity in free space and tanδ is the dielectric loss measured with the sample. The dielectric loss factor is given by ε' tanδ [14].

The variation of real part of the dielectric constant ε' of both ZrO_2 and $ZrTiO_4$ nano particles with respect to frequency at room temperature are as shown in the Fig. 3. It is observed that the samples show high values of dielectric constant for low frequencies, which decreases rapidly with increasing frequency. At higher frequencies the dielectric constant remains independent of frequency due to the inability of electric dipoles to follow the fast variation of the alternating applied electric field, which is the expected behavior in most dielectric materials. The conductivity of grain boundaries contributes more to the dielectric value at lower frequencies [15, 16]. The dielectric constant value of $ZrTiO_4$ shows more value (50) whereas ZrO_2 shows lower value (40). The similar results are reported by Viticoli et al. [17] and also Shanthala et al. [18]. The variation of tanδ with respect to frequency is as shown in the Fig. 4. It is reported that the region between 10^3 - 10^6 Hz is very important for dielectric applications [19]. The rapid decrease in rate of dielectric loss in low frequency is due to the conduction of grain boundary. If more energy is required for hopping of charge carriers, the resultant dielectric loss is high. In high frequency region the dielectric loss decreases slowly due to the conduction of grains, a small energy is required for hopping of charge carriers; as a result the dielectric loss is low. High dielectric loss is for ZrO_2 compare to $ZrTiO_4$. The low dielectric loss value of $ZrTiO_4$ leads to high ac conductivity which is discussed in the next section.

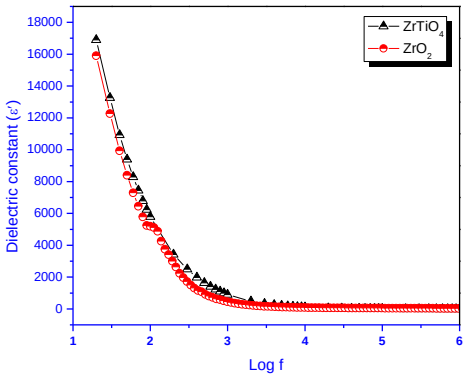

Fig. 3 Dielectric constant responses of ZrO_2 and $ZrTiO_4$ as a function of frequency

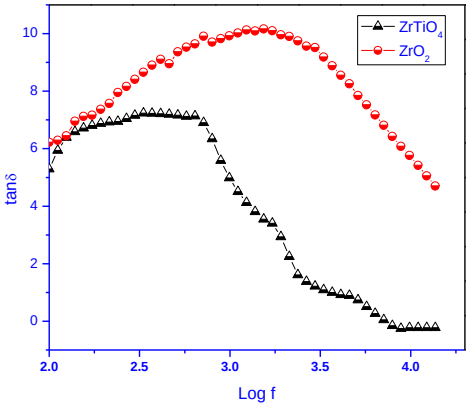

Fig. 4 Dielectric loss responses of ZrO_2 and $ZrTiO_4$ as a function of frequency

https://doi.org/10.30799/jnst.098.18040104

Cite this Article as: H.C. Madhusudhana, S.N. Shobhadevi, B.M. Nagabhushana, M.V. Murugendrappa, R. Hari Krishna, H. Nagabhushana, A comparable study of structural, dielectric and humidity sensing properties of solution combustion synthesized ZrO_2 and $ZrTiO_4$ nano powders, J. Nanosci. Tech. 4(1) (2018) 314–316.

3.4 AC Conductivity

The Fig. 5 Show the variation of AC conductivity with respect frequency at room temperature for both the samples. The AC conductivity of $ZrTiO_4$ was found to be strongly depending on frequency. It has been reported that dispersion in the conductivity is a direct evidence for the hopping motions of charge carriers in neighboring lattice imperfections [20-22]. At low frequencies, conductivity is found to be very small flat peak supporting space charge polarization. The conductivity of $ZrTiO_4$ is found to be of the order of 2.75 x 10^{-4} Scm^{-1} due to increase in oxygen vacancies whereas ZrO_2 found to be of the order of 5.0 x 10^{-15} Scm^{-1}. As frequency increases both the samples conductivity also increases.

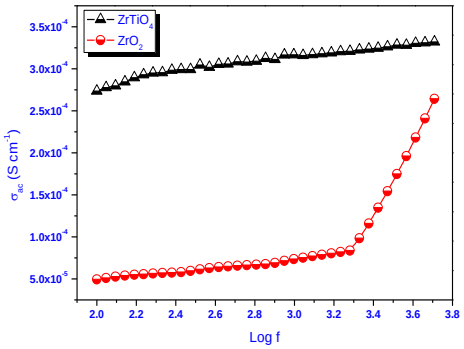

Fig. 5 AC conductivity responses of ZrO_2 and $ZrTiO_4$ as a function of frequency

3.5 Humidity Sensing Study

Fig. 6 shows the RH dependence of resistivity for the sample. The resistance of the $ZrTiO_4$ on exposure to a humid environment decreases with the increase in humidity values from 25% to 85%. The $ZrTiO_4$ react to humidity by decreasing their resistivity, approximately exponential with the relative humidity. The conduction mechanism depends on the surface coverage of adsorbed water. When only hydroxyl ions are present on the oxide surface, the charge carriers are protons, from hydroxyl dissociation, which hop between adjacent hydroxyl groups [23]. The easy dissociation of physisorbed water, due to the high electrostatic fields in the chemisorbed layer, produces H_3O^+ groups. The charge transport occurs when H_3O^+ releases a proton to a nearby H_2O molecule, ionizing it and forming another H_3O^+, resulting in the hopping of protons from one water molecule to another. This process is known as the Grotthuss chain reaction, and it is assumed that it also represents the conduction mechanism in liquid water. This mechanism means that higher resistivity of the oxides is observed at low RH values. This is because mobile protons may arise from the dissociation of the hydroxyl groups or of the water molecules, but the activation energy required to dissociate hydroxyl ions is higher than that necessary to dissociate water molecules.

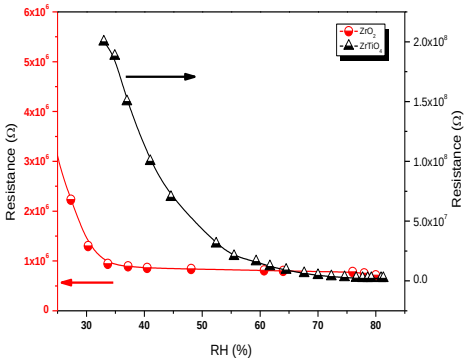

Fig. 6 Variation of relative humidity v/s resistance responses of ZrO_2 and $ZrTiO_4$

A higher carrier concentration is found when more than one layer of physisorbed water molecule is present on the surface. These molecules are singly hydrogen-bonded and form a liquid-like network, which greatly increases the dielectric constant and, therefore, the proton concentration [23]. The dielectric constant value of $ZrTiO_4$ is more and also diectric loss is less from the observed data which leads to increase its humidity sensing property. The improvement in the results shows the presence of more oxygen vacancies which intern increases the absorption of more water molecules [7].

4. Conclusion

ZrO_2 and $ZrTiO_4$ nano powders were prepared successfully by solution combustion method. The characterization like XRD, SEM has been done to confirm the formation of the respective samples. The calculations show the prepared samples are nanoparticles. The obtained nanoparticles are agglomerated and porous in nature. The dielectric study, ac conductivity and humidity sensing properties have been investigated. Compare to ZrO_2 nano powder, $ZrTiO_4$ shows increased dielectric constant (50), superior conductivity (2.75 x 10^{-4} Scm^{-1}) and linear response to humidity atmosphere.

Acknowledgement

H.C. Madhusudhana is grateful to the Principal, Dayananda Sagar Academy of Technology and Management, Bangalore, and also the Director, BMS Academy of Science and Research, Bangalore, for their continuous support and encouragement.

References

[1] R.W. Lynch, B. Morosin, Thermal expansion, compressibility, and polymorphism in hafnium and zirconium titanates, Jour. Am. Ceram. Soc. 55 (1972) 409-413.
[2] M. Leoni, M. Viviani, G. Battilana, A.M. Fiorelloand, M. Viticoli, Aqueous synthesis and sintering of zirconium titanate powders for microwave components, Jour. Eur. Ceram. Soc. 21 (2001) 1739-1741.
[3] J.A. Navio, M. Macias, P.J. Sanchez-Soto, On the influence of chemical processing in the crystallization behaviour of zirconium titanate materials, Jour. Mat. Lett. 11 (1992) 1570-1572.
[4] S.V. Pol, Synthesis of nanocrystalline zirconium titanate and its dielectric properties, Jour. Phys. Colloid Chem. 111 (2007) 2484-2489.
[5] M. Dondi, F. Matteucci, G. Cruciani, Zirconium titanate ceramic pigments: crystal structure, optical spectroscopy and technological properties, Jour. Solid State Chem. 179 (2006) 233-246.
[6] E.L. Sham, M.A.G. Aranda, E.M. Farfan-Torres, J.C. Gottifredi, M. Martinez-Lara, S. Bruque, Zirconium titanate from sol–gel synthesis: thermal decomposition and quantitative phase analysis, Jour. Solid State Chem. 139 (1998) 225-232.
[7] I.C. Consentino, E.N.S. Mucillo, R. Mucillo, Development of zirconia-titania porous ceramics for humidity sensors, Sensor. Actuat. B 96 (2003) 677-683.
[8] H.C. Madhusudhana, S.N. Shobhadevi, B.M. Nagabhushana, B.V. Chaluvaraju, M.V. Murugendrappa, et al., Effect of fuels on conductivity, dielectric and humidity sensing properties of ZrO_2 nanocrystals prepared by low temperature solution combustion method, Jour. Asian Ceram. Soc. 4 (2016) 309-318
[9] M. Dondia, F. Matteuccia, G. Crucianib, Zirconium titanate ceramic pigments: crystal structure, optical spectroscopy and technological properties, Jour. Solid State Chem. 179 (2006) 233–246.
[10] P. Klug, L.E. Alexander, X-ray diffraction procedures (for amorphous and crystalline materials), Wiley, New York, 1954.
[11] G.K. Williamson, W.H. Hall, X-ray line broadening from filed aluminium and wolfram, Acta. Metall. 1 (1953) 22–31.
[12] A.K. Jonscher, Alternating current diagnostics of poorly conducting thin films, Thin Solid Films 36 (1976) 1-20.
[13] M. Thomas, S.K. Ghosh, K.C. George, Characterization of nanostructured silver orthophosphate, Mater. Lett. 56 (2002) 386-392.
[14] N. Yamaoka, $SrTiO_3$-based boundary-layer capacitors, Bull. Am. Ceram. Soc. 65 (1986) 1149-1152.
[15] P. Indradevi, H. Kamalaveni, K. Ramachandran, Dielectric and magnetic behaviour of undoped and Mn-doped ZnSe nanoparticles, Adv. Sci. Eng. Med. 4 (2012) 316–323.
[16] M. Chaari, A. Matoussi, Z. Fakhfakh, Structural and dielectric properties of sintering zinc oxide bulk ceramic, Mater. Sci. Appl. 2 (2011) 765–770.
[17] M. Viticoli, G. Padeletti, S. Kaciulis, G.M. Ingo, L. Pandolfi, C. Zaldo, Structural and dielectric properties of $ZrTiO_4$ and $Zr_{0.8}Sn_{0.2}TiO_4$ deposited by pulsed laser deposition, Mater. Sci. Eng. B 118 (2005) 87–91.
[18] V.S. Shanthala, S.N. Shobha Devi, M.V. Murugendrappa, Ac conductivity and dielectric studies of polypyrrole copper zinc iron oxide nanocomposites, IOSR Jour. Appl. Phy. 8 (2016) 83-89.
[19] W.D. Kingery, Introduction to ceramics, John Wiley and Sons, NewYork, 1976.
[20] S. Narayanan Potty, Abdul Khadar, Dielectric properties of nanophase Ag_2HgI_4 and Ag_2HgI_4-Al_2O_3 nanocomposites, Bull. Mater. Sci. 23 (2000) 361-367.
[21] N.U. Haque, R.A. Hashmi, M.K. Anis, Diffusive barrier in silver phosphate and silver borophosphate glasses, Phys. Stat. Sol. A 142 (1994) 429-433.
[22] D.P. Snowden, H. Saltsburg, Hopping conduction in NiO, Phys. Rev. Lett. 14 (1965) 497-499.
[23] J.H. Anderson, G.A. Parks, Electrical conductivity of silica gel in the presence of adsorbed water, J. Phys. Chem. 72 (1968) 3362-3368.

https://doi.org/10.30799/jnst.098.18040104

Cite this Article as: H.C. Madhusudhana, S.N. Shobhadevi, B.M. Nagabhushana, M.V. Murugendrappa, R. Hari Krishna, H. Nagabhushana, A comparable study of structural, dielectric and humidity sensing properties of solution combustion synthesized ZrO_2 and $ZrTiO_4$ nano powders, J. Nanosci. Tech. 4(1) (2018) 314–316.